

# Current Status and Future Prospective of Neuroimaging for Epilepsy

F. Caranci, F. D'Arco, A. D'Amico, C. Russo, F. Briganti, M. Quarantelli and E. Tedeschi

**Abstract** Although the diagnosis of epilepsy remains mainly clinical, Magnetic Resonance Imaging (MRI) plays a crucial role in the detection of lesions that can cause epilepsy, with high impact on the diagnostic work-up as well as on therapeutic planning. Morphologic MR imaging is still the main technique for identifying lesions responsible for the epilepsy, providing images with high spatial resolution, excellent soft-tissue contrast, and multiplanar view. Quantitative MR image analysis (segmentation, voxel-based morphometry), based on 3D T1-weighted images, offers an objective means of analyzing MR images thereby improving the capability of detecting subtle lesions, often interpreted as negative by qualitative assessment of the morphologic MR imaging. Diffusion tensor imaging allows the quantification of water molecules diffusion and characterizes the degree and direction of anisotropy. Areas of abnormal diffusion, responsible for epilepsy, may be related to occult dysgenesis, or to acquired damage, resulting in neuronal loss, gliosis, and extracellular space expansion; these changes often result in reduced anisotropy and in an increase in mean diffusivity. Magnetic resonance spectroscopy provides information about the biochemical environment of the brain, thereby helping in lateralizing the epilepsy focus. Functional MR imaging is used for lateralizing language functions, and also for surgical planning predicting functional deficits following epilepsy surgery. The interpretation of MR data should always be done by a neuroradiologist expert in the field of epilepsy imaging, trying to correlate the images with clinical and electrophysiological data.

---

F. Caranci (✉) · F. D'Arco · A. D'Amico · C. Russo · F. Briganti · E. Tedeschi  
Department of Advanced Biomedical Sciences, Neuroradiology Unit,  
Federico II University, Naples, Italy  
e-mail: [ferdinandocaranci@libero.it](mailto:ferdinandocaranci@libero.it)

M. Quarantelli  
Institute of Biostructures and Bioimaging, National Research Council, Naples, Italy

© Springer International Publishing Switzerland 2015  
P. Striano (ed.), *Epilepsy Towards the Next Decade*,  
Contemporary Clinical Neuroscience, DOI 10.1007/978-3-319-12283-0\_7

## Introduction

Modern neuroimaging techniques have had a major impact on our understanding of epilepsy. They provide high degree anatomical resolution and functional/metabolic information about the epileptic lesion, contributing to the proper classification of several epileptic disorders.

Magnetic Resonance Imaging (MRI) is a powerful tool in identifying epileptogenic tumors (gangliogliomas, DNETs, hypothalamic hamartoma, pleomorphic xanthoastrocytoma, etc.), vascular malformation (cavernous hemangiomas), severe developmental causes of intractable epilepsy (hemimegalencephaly, schizencephaly) and other syndromes that can lead to intractable seizures (neurocutaneous syndromes, such as Sturge-Weber syndrome and tuberous sclerosis). By using modern MR systems, that provide high image resolution and multiparametric reconstructions, it is often possible to recognize also small anatomical substrates responsible for epilepsy such as focal cortical malformations (focal cortical dysplasia, heterotopia, polymicrogyria) and hippocampal sclerosis. These are the most common causes of epilepsy, but they can be depicted only with a dedicated MR protocol; the sensitivity of MR imaging for such small structural abnormalities also depends on the experience of the interpreting physician (Widjaja and Raybaud 2008).

However, MRI is not always able to detect structural abnormalities in patients with seizures. Considering large case series of patients with intractable epilepsy, MRI showed a sensitivity from 82 to 86% in identifying the epileptogenic substrate (Scott et al. 1999, Berg et al. 2000), while in children with a new diagnosis of epilepsy MRI detected epileptogenic substrates in only 13% of cases (Bronen et al. 1996).

In recent years, new advanced MR imaging such as diffusion tensor imaging (DTI), magnetic resonance spectroscopy (MRS), quantitative MR imaging, functional MR imaging (fMRI), together with nuclear medicine procedures (positron emission tomography—PET and single-photon emission computed tomography—SPECT) have increased the sensitivity in the diagnosis of epileptic anatomical substrates and the knowledge of the mechanisms of seizures; moreover, in pre-surgical evaluation of epilepsy, the combined use of multiple imaging modalities for precise localization of the epileptogenic focus provides a better planning and ensures better surgical outcome.

The aim of this chapter is to provide an overview of structural and advanced imaging of epilepsy focusing on the best protocol tailored to the clinical diagnosis; in the second part, the MR appearance of the most important causes of epilepsy will be schematically described.

## *Imaging Modalities*

### **Computed Tomography**

Computed tomography (CT) uses ionizing radiation and can generate excellent hard tissue imaging contrast with moderately good soft tissue resolution. The advantages

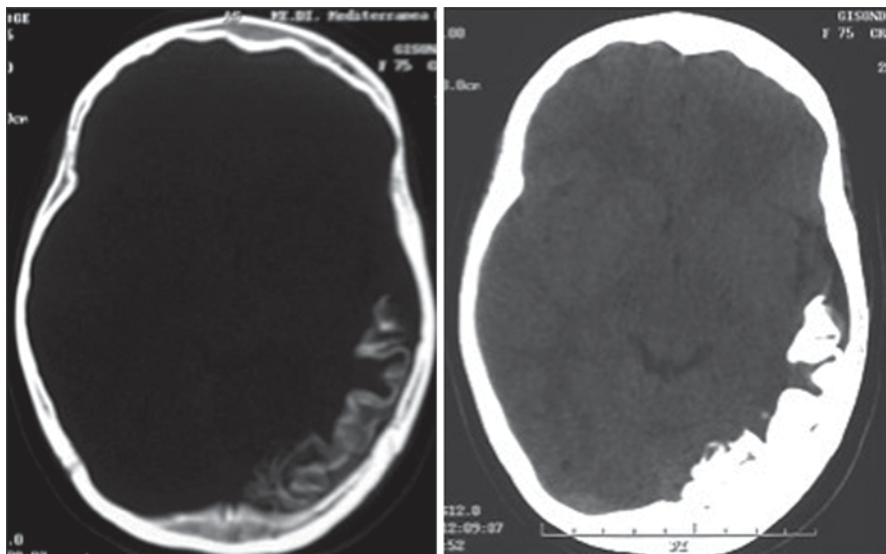


**Fig. 1** CT scan of a patient with Sturge-Weber syndrome. Cortical and subcortical “tram-track” calcifications in the *left* posterior hemisphere are evident

of CT are wide accessibility, low cost, high speed (last CT generation can obtain a complete brain scan in few seconds) and thus it is considered a reliable brain imaging modality for most patients especially in emergency. CT can easily identify hemorrhage, infarctions, gross malformations, ventricular system pathologies, and lesions with underlying calcification (Trishit Roy and Alak 2011).

The sensitivity of CT in patients with epilepsy has not been found to be higher than 30% in unselected patient populations (Hankey et al. 1989; Wyllie et al. 1989; Gastaut and Gastaut 1979). This is due to the low resolution of CT for detecting mesial temporal lobe sclerosis (the most common epileptogenic substrates in adults) and temporal epileptogenic tumors (such as gangliogliomas or DNETs).

The use of CT for patients with epilepsy has been greatly diminished by the availability of MRI. Even if sometimes CT scan is used in neonates and infants following a pathological ultrasound (Hankey et al. 1989; Wyllie et al. 1989), it is always better to use, if available, MRI (under sedation) to better characterize the brain abnormalities.

Moreover, the role of CT in the diagnosis of tuberous sclerosis, Sturge-Weber syndrome (Fig. 1), and other pathologies with intracranial calcifications remains complementary, because MRI provides more information (noncalcified tubers).

CT can be still considered the technique of choice in the postoperative evaluation of patients undergoing surgery for uncontrolled seizures, because it can rapidly detect early complications of surgery such as hemorrhage, hydrocephalus, and major structural changes (Trishit Roy and Alak 2011).

**Table 1** Epilepsy MRI protocol.

GE 3D T1	Isotropic voxel < 1 mm
Axial FLAIR & T2	2–4 mm slice thickness
Coronal FLAIR/HR T2	In temporal lobe epilepsy: coronal sections perpendicular to the long axis of hippocampus, axial sections parallel to the long axis of hippocampus
3D FLAIR	Suspect of cortical dysplasia
Axial or coronal GE T2*/axial SWI	Suspect of cavernous hemangioma, occult calcified lesions
DWI/ADC	Water restriction: cytotoxic edema
Contrast-enhanced T1	Brain tumors, Sturge-Weber syndrome

### Structural Magnetic Resonance Imaging

MRI is the imaging procedure of choice in the investigation of patients with epilepsy. The advantages of MRI include the use of nonionizing radiation, high sensitivity and higher specificity than CT, multiplanar imaging capability, improved contrast of soft tissue, and high anatomical resolution. The sensitivity of MRI in detecting abnormalities in patients with epilepsy is strictly dependent on the type of pathologic substrate of the epilepsy, on the MRI protocol used, and on the experience of the interpreting physician (Widjaja and Raybaud 2008). Clinical data and electroencephalographic (EEG) findings should always guide the interpretation of MR images.

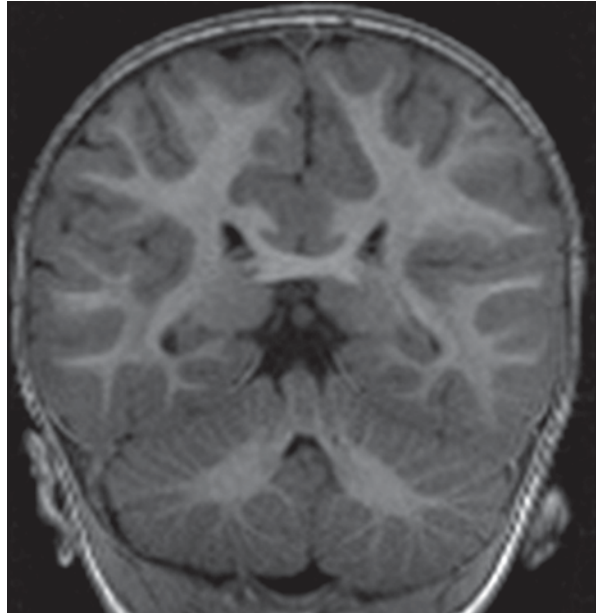
An optimal MRI protocol in an epileptic patient should use sequences with the minimum slice thickness, covering the whole brain and providing a high contrast resolution (that is the ability to distinguish between differences in intensity in an image) (Opplet 2006).

The use of 3 Tesla MR scanners, providing a better image resolution, improves the evaluation of patients with focal epilepsy when compared to 1.5 Tesla scanners (Mueller et al. 2011), with an important impact in the correct presurgical identification of the epileptic focus and thus in the treatment.

A dedicated MRI protocol should include (De Cocker et al. 2012, Table 1):

1. **3D T1 images with  $\leq 1.5$  mm slice thickness**, useful in assessing cortical thickness and gray/white matter interface (Fig. 2) and reformattable in any orthogonal or nonorthogonal planes (Widjaja and Raybaud 2008). In order to better evaluate the cortical thickening in case of focal cortical dysplasia (FCD), some authors suggest to add curvilinear reformatting using 3D data (Widjaja and Raybaud 2008; Montenegro et al. 2002). The complexity of the brain gyration is not perfectly studied using the orthogonal planes only, since the plan of analysis can be oblique to some gyri, thereby leading to apparent cortical thickening and thus to a false-positive diagnosis of FCD. In these cases, a curvilinear reconstruction can be useful to clarify the nature of a suspect area of cortical malformation detected on orthogonal planes.

**Fig. 2** 3D T1 weighted image reformatted on coronal plane, with excellent *gray/white* matter contrast



In <2 year-old children, 3D T2 w images are preferred to better evaluate the white matter because of the still incomplete myelination;

2. **T2 and FLAIR images** in axial and coronal planes, necessary to detect subtle cortical and subcortical hyperintensities (focal cortical dysplasia, small tumors, gliosis, hippocampal sclerosis); it is important to note that the best way to detect the presence of hippocampal sclerosis is to orientate the axial T2 and FLAIR sections parallel to the hippocampal axis, and the coronal slices perpendicular to it;
3. **T2\* gradient echo or susceptibility weighted images (SWI) images**, helpful for identifying hemoglobin breakdown products as in post-traumatic changes and cavernomas, or when searching calcifications in tuberous sclerosis, Sturge-Weber syndrome and gangliogliomas;
4. **Contrast-enhanced T1 w images** (at least in two orthogonal planes) in case of brain tumors or Sturge-Weber syndrome;
5. **Diffusion weighted imaging** for the detection of foci of diffusion restriction consistent with cytotoxic edema or increased cellularity.

Some authors have proposed the use of **Double Inversion Recovery pulse sequence (DIR)** in case of suspected hippocampal sclerosis (Li et al. 2011). This sequence provides two different inversion pulses, which attenuates the cerebrospinal fluid (CSF) as well as the whole white matter, thus achieving a superior delineation between gray and white matter (Wattjes et al. 2007); it is considered superior to conventional MR sequences in the evaluation of subtle intensity changes in hippocampal sclerosis (Li et al. 2011).

**Fetal MRI** is a relatively new technique that provides increased diagnostic accuracy in the evaluation of fetal brain. This technique allows to detect small brain malformations very early during pregnancy, even not detectable by ultrasonography (US): a case of abnormal cortex and heterotopic gray matter has been described in a 24 weeks old fetus (Iaccarino et al. 2009).

### **Quantitative MR Imaging**

Pathological examination of surgical specimens obtained in patients with intractable focal epilepsy and in whom the qualitative assessment of structural MR images was inconclusive, has shown the presence of subtle lesions such as loss of neurons, gliosis and microdysgenesis (cortical dyslamination and cytoarchitectural abnormalities) (Widjaja and Raybaud 2008; Al Sufiani and Ang 2012).

Quantitative volumetric analysis of MR images, usually performed by 3D T1-weighted images, can increase the sensitivity of MR in detecting epileptogenic foci especially in case of mesial temporal lobe epilepsy (TLE).

Volume reduction in hippocampus and in extrahippocampal regions has been demonstrated in mesial TLE (Guimaraes et al. 2007): a recent meta-analysis of voxel-based morphometry (VBM) studies on unilateral refractory temporal lobe epilepsy (Widjaja et al. 2012) showed significant reductions in ipsilateral mesio-temporal structures and in bilateral thalamus in both refractory left TLE and refractory right TLE. Bilateral abnormalities of frontal lobe and right cingulate gyrus were also found in the refractory left TLE patients, whereas right insular atrophy was found in the refractory right TLE group. Thus, quantitative MR imaging can depict the presence and laterality of hippocampal atrophy in TLE with accuracy rates, that may exceed those achieved with visual inspection of clinical MR imaging studies. Quantitative MR imaging can therefore enhance standard visual analysis, providing a useful and viable means for translating volumetric analysis into clinical practice (Farid et al. 2012).

Volumetric abnormalities affecting the thalamus and the frontal lobe were also found in generalized epilepsy (Widjaja et al. 2012). Moreover, in children with new-onset seizures a significant reduction in cortical thickness has been reported (Widjaja et al. 2012), while no significant differences in hippocampal and thalamic volumes were observed, suggesting that structural changes in cortical gray matter may predispose the patients to seizures while other changes can be due to the cumulative effects of recurrent seizures.

### **Diffusion Tensor Imaging (DTI)**

Diffusion MRI is a MR modality that allows the mapping of the diffusion process of molecules of water in human tissues.

In the brain, water diffusion is restricted by myelin, membranes and macromolecules; in the white matter, the diffusion is mainly parallel to the white matter tracts

and minimally perpendicular to them. This can explain the concept of **anisotropy** that expresses the asymmetric diffusion of water molecules in three dimensions.

Diffusion Tensor Imaging (DTI) allows the calculation of the degree and of the direction of anisotropy (Widjaja and Raybaud 2008).

From a mathematical point of view, DTI is a model of an ellipsoid that has a principal long axis and two more small axes. These three axes are perpendicular to each other and cross at the center point of the ellipsoid: the axes in this setting are called **eigenvectors** and the measures of their lengths **eigenvalues**; eigenvectors are the directions of the diffusion while each eigenvalue represents the magnitude of diffusion along each axis.

From a practical point of view, some diffusion parameters can be calculated in order to obtain information about the microstructural features of brain tissue: (1) the mean diffusivity (MD), that provides an evaluation of the magnitude of the diffusion motion in a voxel region and is measured in square millimeters per seconds; (2) the fractional anisotropy (FA), that is a scalar value between 0 and 1 that describes the values of the anisotropy. A FA value of 0 represents absence of anisotropy (the diffusion is isotropic) as in a perfect sphere, while a values of 1 represents maximal anisotropic diffusion.

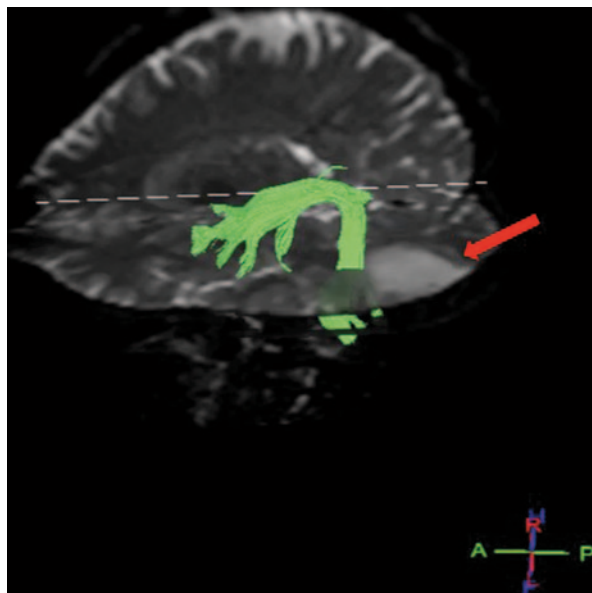
Most acquired lesions and malformations of cortical development cause microstructural changes in the brain (reduction in cell density, impairment of normal myelin architecture, expansion of extracellular space), leading to reduced FA and increased MD (Widjaja and Raybaud 2008).

Several studies based on DTI in epileptic patients showed abnormal FA and MD.

Reduced FA was found in the white matter both ipsilateral and contralateral to the seizure focus (Widjaja et al. 2014); reduced FA and increased MD was found adjacent to cortical malformations visible on MR (Eriksson et al. 2001) and also beyond the margins of malformations detectable on MR imaging (Widjaja and Raybaud 2008) ‘consistent with the EEG changes extending beyond the boundaries of focal cortical dysplasia visible on imaging, allowing a better surgical outcome’ or distant from visible malformation of cortical development (Dumas de la Roque et al. 2005). Finally, significantly decreased FA values were observed in the cerebellum of patients with generalized tonic-clonic seizures (Li et al. 2010). The areas of abnormal diffusion detected using DTI in epileptic patients are thought to be caused by damage of the brain microstructure (neuronal loss, extracellular space expansion and gliosis) related to dysgenesis, acquired injuries or secondary to repeated seizures. For these reasons, DTI is considered a powerful tool in studying the anatomical substrates of epilepsy as well as the microstructural changes related to seizures. However the complexity of the analysis of the DTI data and the time-consuming post-processing limit the use of DTI parameters in routinary MR studies.

Finally, it is possible to obtain virtual 3D maps of eloquent white matter tracts (such as cortico-spinal tracts, optic radiations and arcuate fasciculus) by using DTI raw data (diffusion tensor tractography, Fig. 3); this technique is very useful in pre-operative evaluation of epileptogenic lesions since it allows to localize white matter tracts and to assess their spatial relationship to the lesions (Lee et al. 2013).

**Fig. 3** Diffusion tensor tractography. 3D reconstruction of the left arcuate fasciculus (*green*) and its relationship with an epileptogenic tumor of the posterior temporal lobe (*red arrow*)



### Magnetic Resonance Spectroscopy (MRS)

Magnetic resonance spectroscopy (MRS) is an analytical technique capable of evaluating the biochemical environment of the brain, and used to complement structural MRI in the characterization of tissues.

In clinical practice MRI uses signals from hydrogen protons ( $H^1$ ) to determine the relative concentrations of target brain metabolites (Fig. 4). The most important brain metabolites assessed by MRS are: N-acetylaspartate (NAA), choline (Cho), creatine (Crea), lipids (Lip), lactate (Lac), glutamate-glutamine (Glx), Alanine (Ala) and myoinositol (Myo).

**NAA** is normally present in neurons and in axons and thus reflects the number of functioning neurons. Decrease in NAA levels indicates neuronal tissue loss or damage and axonal integrity loss.

**Cho** is a major component of cell membranes and the concentration of this metabolite provides information about cell density, membrane turnover and degree of myelination. An increase in Cho concentration indicates increase in cell production and/or membrane breakdown (brain tumors, demyelination).

**Crea** is a marker of cellular metabolism; it can be reduced in some pathological conditions such as lack of blood supply, but it can also be increased in response to cranio-cerebral trauma. However, because the concentration of Crea is relatively constant and is considered the most stable cerebral metabolite, it can be used as internal reference for calculating metabolite ratios.

**Lac** is not normally visible in MRS; when present, it indicates anaerobic metabolism (ischemia, hypoxia, necrotic brain tumors).



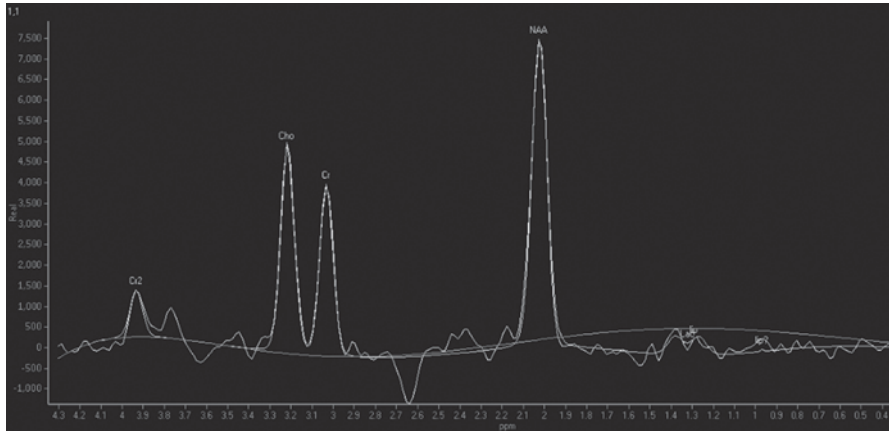


**Fig. 4** Normal MRS of the brain (*single voxel, long TE*), placed in the white matter of the parietal lobe in a normal subject. Note the normal peak of NAA, higher than the Cho peak, and the absence of the pathological peaks of Lac and Lip

**Lip** are components of cell membranes normally not visualized on MRS. Lip peaks can be seen when there is cellular membrane breakdown or necrosis such as in metastases or primary malignant tumors.

**Glx** concentration reflects the glutamate concentration in glutamatergic neurons.

**Ala** is thought to play a role in citric acid cycle; increase of Ala concentration occurs in oxidative metabolism defects and in meningiomas.

**Myo** is a glial marker because is present almost exclusively in astrocytes. Myo may represent a marker of myelin degradation: elevated Myo is found in inflammation, gliosis, astrocytosis and in Alzheimer's disease.

Abnormalities on MR spectroscopy, such as reduced NAA and increased Cho levels, ipsilateral to EEG focus in patients with normal MRI findings (Widjaja and Raybaud 2008), have been used for lateralizing TLE: these results are consistent with loss of neurons, increased glial cells and neuronal dysfunction that are the pathological substrates of epilepsy. Another finding in TLE is high level of Glx, ipsilateral to the seizure onset, also in patient with "normal" MR (Savic et al. 2000).

For these reasons, MRS can play an adjunctive role in the presurgical evaluation of medically refractory TLE: by using reduced NAA/Cr ratios as a marker of neuronal loss, MRS agreed with the lateralization determined by EEG better than MR imaging volumetry alone (Caruso et al. 2013).

On the other hand, in extratemporal lobe epilepsy MRS was less specific in lateralizing the epilepsy focus (Widjaja and Raybaud 2008; Striano et al. 2008).

Abnormal metabolite concentrations have been found in patients with focal cortical dysplasia (FCD), correlating with the frequency of seizures, while normal NAA ratios have been found in patients with polymicrogyria and gray matter heterotopia (Widjaja and Raybaud 2008).

It is important to highlight that in case of FCD an abnormal spectrum is expected, because this is a malformation secondary to abnormal neuronal proliferation and differentiation.

Conversely, in case of polymicrogyria the neurons are more mature compared to FCD because this is a malformation related to abnormal cortical organization, while in gray matter heterotopias, a malformation due to abnormal migration, there is an increased number of neurons in an abnormal location. These features can explain the normal MRS findings in case of polymicrogyria and heterotopia.

## Functional MR Imaging (fMRI)

Functional MRI (fMRI) is based on the quantification of the increased blood flow in areas of increased neuronal activity: this leads to a decreased oxyhemoglobin/deoxyhemoglobin ratio that is detectable using fMRI sequences (so called “BOLD” effect).

This imaging technique can be used for mapping neuronal activity during visual, language and sensorimotor activities in presurgical planning for epileptogenic lesions.

The understanding of the relationship between the areas of major neuronal activity and the epileptogenic lesion is useful to predict the post-surgical outcome and it is used for this purpose together with the location of main white matter tracts obtained using tractography.

In particular, a major role of fMRI is in lateralizing language functions in case of lesions that are close to language areas of the brain and in showing sensorimotor areas in case of lesions close to perirolandic cortex as this can predict possible language or sensorimotor deficits after surgery (Fig. 5).

In order to elicitate the BOLD effect numerous motor, sensory, verbal fluency and language comprehension tasks have been proposed and are widely used in clinical practice.

fMRI has also been used to probe the integrity of the functional connections among different brain regions, which can be detected when a subject is not performing an explicit task (resting-state fMRI, RS-fMRI) (Biswal 2012). Resting-state networks (RSNs) are the brain regions that exhibit spontaneous low-frequency synchronous fluctuations and represent brain functional connectivity. In particular, region-wise functional connectivity among the frontal, parietal, and temporal lobe, is normally present across the so-called Default-Mode Network (DMN, Fig. 6).

On the basis of PET, SPECT and EEG studies, epilepsy has been postulated to be a disorder of neuronal networks (Widjaja et al. 2013). Several studies have evaluated RSNs in patients with TLE epilepsy, generalized seizures, absence epilepsy and frontal lobe epilepsy revealing abnormal connectivity in different RSNs and negative correlation with epilepsy duration (Widjaja et al. 2013; Luo et al. 2011).

Therefore resting-state fMRI seems to be a promising technique to understand the pathological changes in neuronal connectivity in patients with different forms of epilepsy.

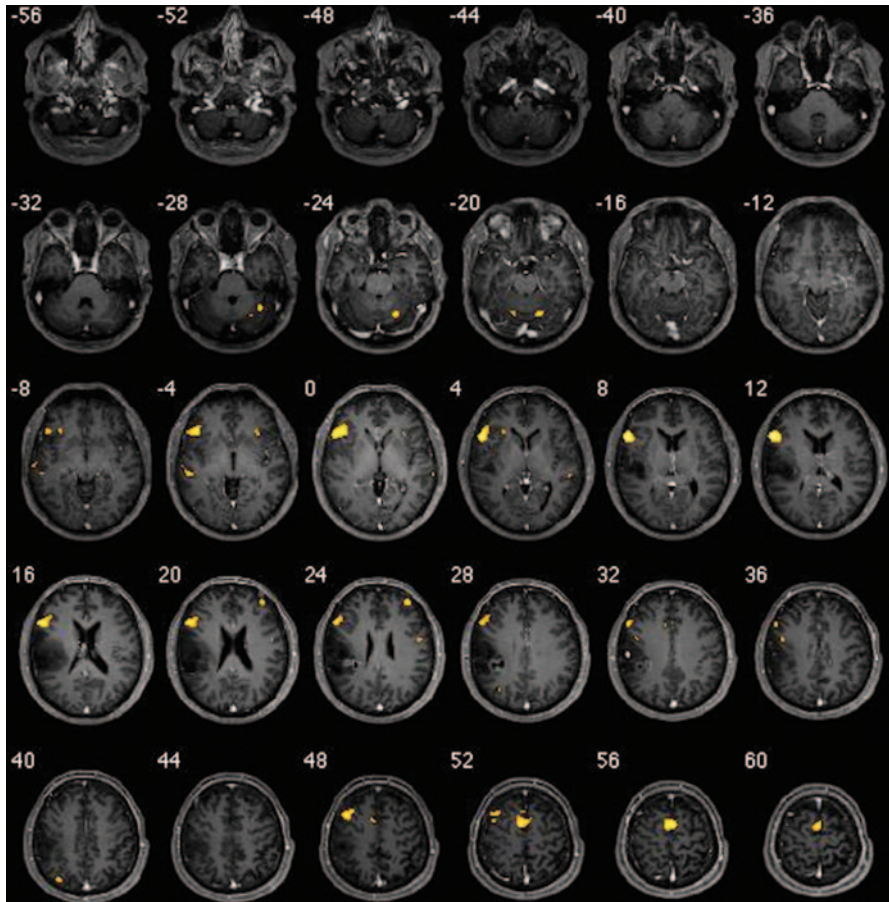


**Fig. 5** fMRI (language task) after surgical excision of an epileptogenic tumor. Close relationship between the post-surgical cavity and the activation of the Broca's area, in the *left* inferior frontal gyrus

### Positron Emission Tomography (PET)

The role of interictal PET with fluorodeoxyglucose (FDG-PET) is to determine the lateralization of the epileptic focus in the presurgical assessment of intractable epilepsy (Widjaja and Raybaud 2008). The spatial resolution of this technique is around 4 mm, therefore the images should be viewed side-by-side with MRI, or, even better, co-registered with MRI (Chugani et al. 1990).

The area of most severe glucose hypometabolism is typically located in the site of ictal onset; however, the volume of hypometabolism is often widespread. This is the reason why FDG-PET hypometabolism can be used to lateralize the side of seizure onset and to determine the prognosis for complete seizure control only when it correlates with EEG recordings, MRI and/or clinical data (Widjaja and Raybaud 2008).

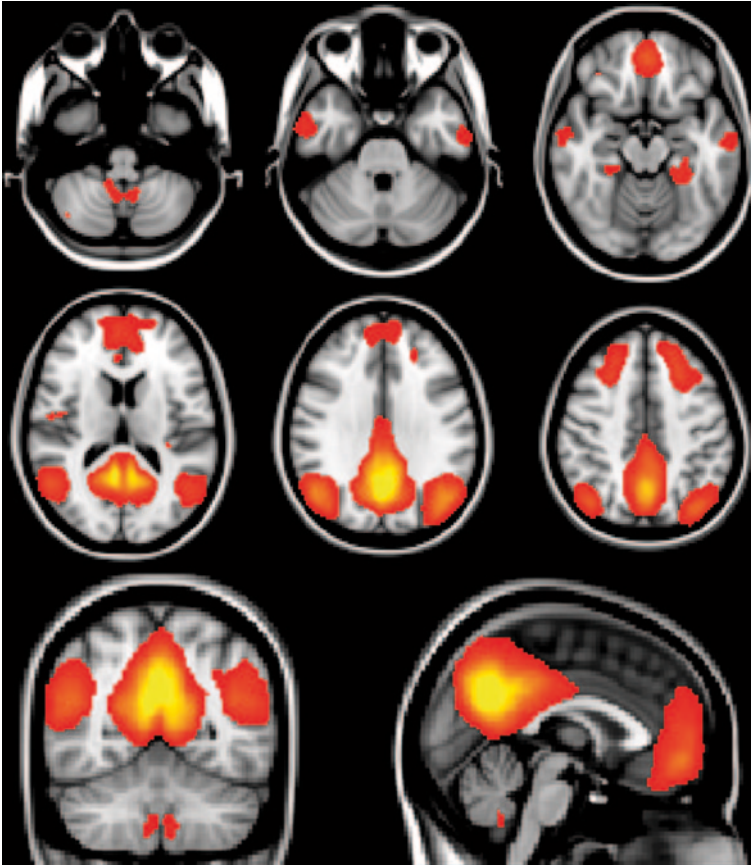


**Fig. 6** Color map of the DMN as detected by Independent Component Analysis of the Resting-State fMRI data acquired at 3T in a group of 20 healthy subjects. The main components of the DMN in the inferior parietal regions, posterior cingulate and adjacent precuneus, as well as medial temporal and prefrontal cortices can be appreciated as *yellow-red* areas

In mesial TLE, interictal studies show hypometabolic areas in the epileptogenic regions in approximately 80% of patients; the changes, however, are more extensive than the structural and EEG abnormalities and may involve the lateral temporal lobe, ipsilateral frontal lobe, ipsilateral parietal lobe and basal ganglia (epileptic network) (Widjaja and Raybaud 2008; Pittau et al. 2014).

In extratemporal lobe epilepsy, interictal PET-FDG studies are less useful, especially if the MRI is normal and the scalp EEG is nonfocal. However, PET has been reported to be more sensitive in neonates and infants with focal seizures because of a possible developmental malformation. This is particularly the case in patients with infantile spasms and focal features on EEG. PET has also improved the understanding of the pathophysiology of infantile spasms by demonstrating activation of cortical regions, brainstem, and lenticular nuclei (Chugani et al. 1990).

The mechanisms underlying this hypometabolism in the epileptogenic cortex are still unresolved: it is thought that FDG-PET distribution reflects mainly synaptic activity, rather than cellular loss (Pittau et al. 2014).

In conclusion, the high sensitivity of MRI in detecting the anatomical substrates of epilepsy has diminished the role of FDG-PET in the presurgical investigation of such patients. Nevertheless, when MRI is normal, PET can be indicated to aid in localization or can be used as a guide for reviewing MRI in search for subtle overlooked cortical dysplasia or other epileptic substrates.

### **Single Photon Emission Computed Tomography (SPECT)**

SPECT has been utilized in patients with epilepsy in the past decades, mainly using diffusible tracers for assessing brain perfusion (such as hexamethylpropylene amine oxime or ethyl cysteinyl dimer). The main role of SPECT is to localize the epileptogenic zone when imaging and other non-invasive exams are unable to identify the site of seizure onset (Widjaja and Raybaud 2008).

Numerous studies using dynamic and static SPECT techniques in the ictal and interictal state have been published.

The ictal SPECT examination can identify focal hyperperfusion, while the interictal examination demonstrates hypoperfusion in the corresponding epileptogenic region. However, the diagnostic value of the interictal SPECT alone is poor, and a combined ictal/interictal SPECT study should be performed, possibly with subtraction of interictal images from the ictal ones and then coregistration with MR images, in order to achieve a better anatomical definition of the site of the seizure (Widjaja and Raybaud 2008).

## ***Imaging of Epileptogenic Diseases***

### **Mesial Temporal Sclerosis**

The most useful MR sequences for detecting mesial temporal sclerosis (MST) are **coronal IR and/or 3D T1 weighted images**, that show a shrunken hippocampus associated with a widening of adjacent temporal horn and choroid fissure, and **coronal FLAIR (or T2)** that shows an increased hyperintensity and loss of the internal architecture of the involved hippocampus (Fig. 7a). Using 3D T1 weighted images it is also possible to detect the atrophy of the fornix and of the mamillary body ipsilateral to the affected hippocampus (Osborn 2013; Caranci et al. 2007; Iaccarino et al. 2009).

MRS typically shows a reduction of NAA (Fig. 7b) related to the neuronal loss both in hippocampal and extrahippocampal regions, while Cho and Cr are unchanged (Mueller et al. 2011).

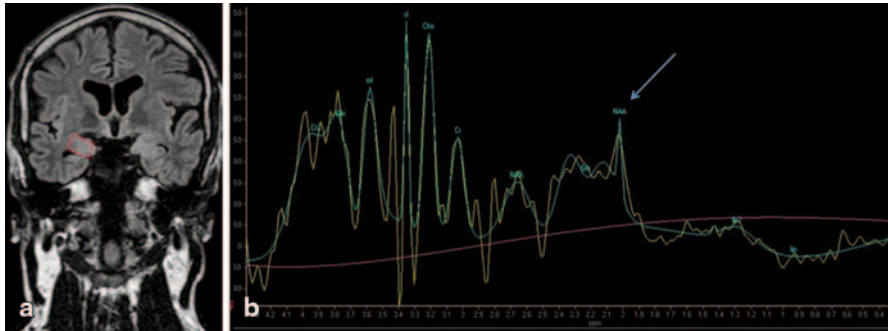


**Fig. 7** Mesial temporal sclerosis. Coronal FLAIR image **a** shows mild atrophy and hyperintensity of the right hippocampus (*red box*); MRS **b** demonstrates a reduction of the NAA peak (*blue arrow*)

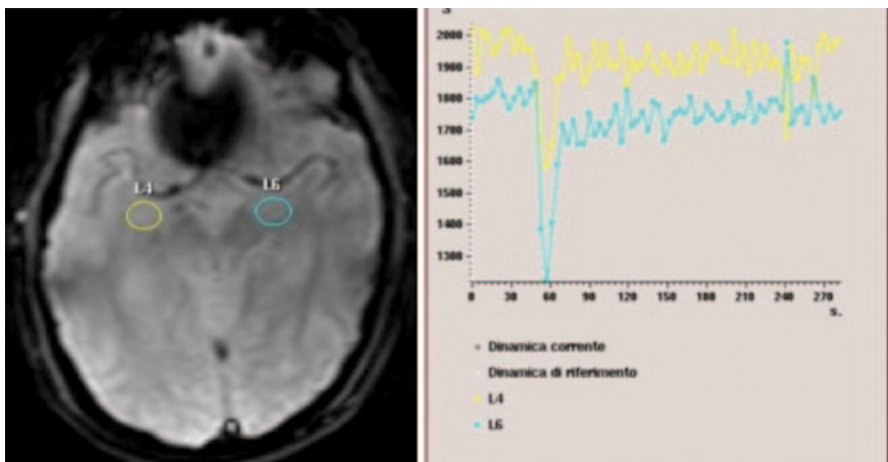


**Fig. 8** Mesial temporal sclerosis. Quantitative PWI analysis in the same patient of Fig. 7 shows reduced perfusion in the right hippocampus (*yellow*) compared with the controlateral side (*blue*)

DWI shows increased diffusivity (high ADC values), while perfusion-weighted images show an interictal hypoperfusion of the affected side compared with the contralateral (Wolf et al. 2001; Fig. 8).

Volumetric analysis of hippocampi, parahippocampal giri and entorhinal cortex is used to quantify temporal lobe abnormalities in comparison with healthy controls; this is very useful in case of bilateral MST (Keller and Roberts 2007).

Finally, fMRI can be used in pre-operative planning to assess the language lateralization and the risk of memory disorders.

FDG-PET typically shows hypometabolism in the affected temporal lobe in the interictal phase and is a very sensitive imaging modality for diagnosis of MTS (Osborn 2013).

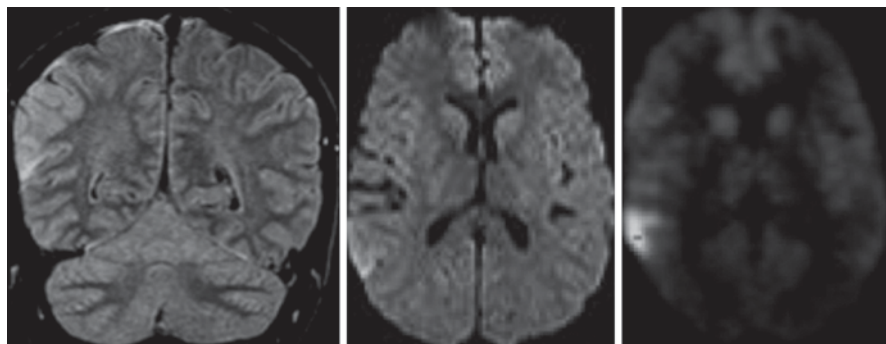


**Fig. 9** Status Epilepticus. Coronal FLAIR image (a) showing hyperintensity and swelling of the temporo-occipital cortex; axial DWI (b) and FDG-PET (c) showing regional diffusion restriction and hypermetabolism, respectively

The differential diagnosis is with diseases that can cause seizures and FLAIR/T2 hyperintensity in the temporal lobe, including status epilepticus, characterized by gyral swelling instead of shrinking, and DWI/ADC restriction, and temporal lobe low grade glioma, that also causes mass effect instead of volume loss.

### Status Epilepticus

MR findings of status epilepticus (SE) include T2/FLAIR hyperintensity and gyral swelling involving the gray matter (cortex, thalami, hippocampi) in a non-vascular distribution with sparing of both subcortical and deep white matter (Fig. 9).

Contrast enhanced T1 weighted images usually do not show any enhancement, only sometimes a variable enhancement of the gray matter; the acute phase is typically also characterized by restricted diffusion on DWI (low ADC values), hyperperfusion on PWI and hypermetabolism on FDG-PET.

Most of the MR findings in SE normalize in few days, however some patients can have permanent damage such as cortical laminar necrosis and brain atrophy (Osborn 2013; Milligan et al. 2009).

The major differential diagnosis is with cerebral ischemia, that typically shows a vascular distribution and involves both gray and white matter.

### Focal Cortical Dysplasia

MR features of focal cortical dysplasia (FCD) depend on its type. The most common is FCD type II b, located most often at the bottom of a sulcus and histopathologically characterized by altered cortical layering, dysmorphic neurons and balloon cells. MRI of FCD II b shows: (1) focal cortical thickening (Fig. 10); (2) blurred interface between gray and white matter; (3) subcortical T2/FLAIR hyperintensity;

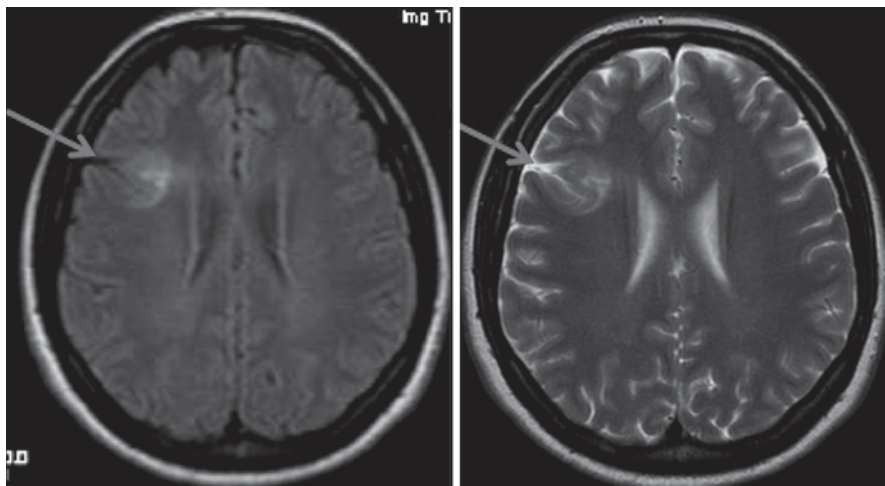


**Fig. 10** Focal Cortical Dysplasia. Axial FLAIR **a** and T2 **b** images show thickening of the cortex at the bottom of a frontal sulcus with subcortical white matter hyperintensity (*arrows*)

(4) “transmantle sign” (not always present), i.e. a stripe of T2/FLAIR hyperintensity extending from the subcortical area to the margin of the ventricle due to a defect of neuronal migration (Fig. 11; Colombo et al. 2009).

CT scan is only able to detect the presence of calcifications associated with FDC (possible but rare).

The differential diagnosis of FCD includes cortically-based tumors associated with seizures such as dysembryoplastic neuroepithelial tumors (DNET), gangliogliomas and oligodendrogliomas.

MRS has been proposed as a reliable tool for differentiating FCD from a neoplasm, showing a reduced NAA/Cr ratio and no elevation in Cho/NAA (Widjaja and Raybaud 2008; Caruso et al. 2013) in the former.

Other advanced techniques can be used in the assessment of FDC: PWI shows increased perfusion in the area of FCD (Wintermark et al. 2013), while DTI can demonstrate microstructural abnormalities of the white matter extending beyond the main lesion seen on MRI (Widjaja and Raybaud 2008; Fonseca Vda et al. 2012).

### Polymicrogyria and schizencephaly

Polymicrogyria (PMG) is a malformation due to abnormal late neuronal migration and cortical organization. PMG can be unilateral or bilateral and is located more often around the sylvian fissure (particularly in its posterior part), although it has been reported in any part of the cerebral cortex (Barkovich 2010).

MR findings of PMG include at least three possible aspects of the cortex (Barkovich 2010):



**Fig. 11** “Transmantle” sign. T2w image shows a hyperintense stripe extending from the subcortical area to the margin of the ventricle due to a defect of neuronal migration (*red arrow*)



1. cortical surface with multiple small, delicate gyri;
2. thick and bumpy cortex;
3. “paradoxically” smooth cortex.

Moreover, an irregular gray/white matter interface is always present (Fig. 12a).

Sulci at the level of PMG are shallow or flat, and T2w and post-contrast T1w images can show enlarged pial veins overlying PMG (Barkovich 2007).

MRS shows relatively normal NAA ratios (Widjaja and Raybaud 2008). Using DTI it is possible to demonstrate abnormalities in the white matter underlying the polymicrogyric areas (Fig. 12b; Bonilha et al. 2007).

CT can show periventricular calcifications in case of PMG associated with congenital cytomegalovirus infection.

FDG-PET in the interictal phase can show hypometabolism in the PMG and surrounding areas (Fig. 12c; Barkovich 2007).

**Schizencephaly** is a disorder of neuronal migration and cortical organization, consisting in an abnormal hemispheric cleft that connects the ventricle with the subarachnoid space. Typical feature of schizencephaly is dysplastic gray matter lining its lips (PMG, pachigyria or normal-sized gyri).

### Heterotopic Gray Matter

Heterotopic foci of gray matter are collections of nerve cells in abnormal locations secondary to the arrest of normal migration of neurons along the radial path between the ventricular walls (ependyma) and the subcortical regions (Bentivoglio et al. 2003).

Heterotopic gray matter may have different morphologies, but the most common are (Guerrini et al. 2006):

1. subependymal (periventricular nodular heterotopia, PVNH);
2. focal subcortical (FSH).

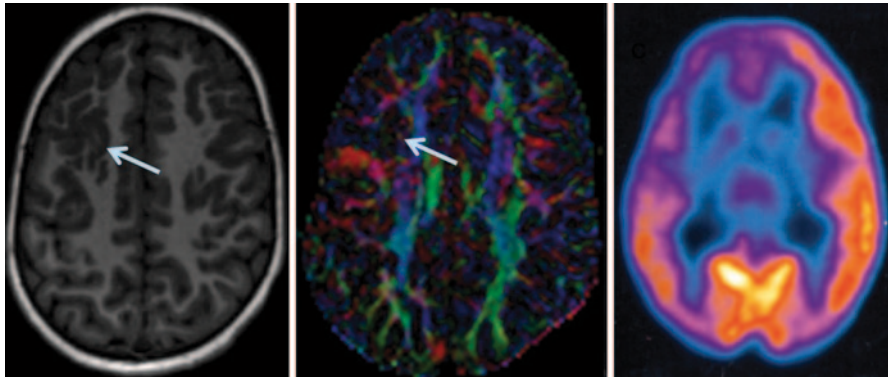


**Fig. 12** Polymicrogyria. Axial 3D T1w (a) and DTI color map (b) show PMG in the left frontal lobe with associated abnormalities in the underlying white matter (arrows). FDG-PET (c) shows area of hypometabolism in the left frontal lobe

In both types, CT may rarely show dysplastic calcifications.

On MRI sequences heterotopic gray matter foci are always isointense to gray matter with distinct or blurred margins. They do not enhance after administration of contrast agents (Barkovich and Raybaud 2012).

PVNH are usually smooth, round or ovoid masses sometimes exophytic, protruding into the adjacent lateral ventricle (Wieck et al. 2005; Fig. 13).

Focal subcortical heterotopia are usually large and heterogeneous masses, which may appear as multinodular or composed of swirling, curvilinear bands of gray matter, extending from the cortex to the ventricles, and often containing blood vessels and CSF (Lim et al. 2005).

MRS may show elevated creatine and choline with normal NAA (Marsh et al. 1996), but the NAA/Cr ratio may be variable, ranging from normal to low (Li et al. 1998).

PWI, in some cases, can identify areas of hyperperfusion, and fMRI usually shows activated areas responding to stimuli just like the normal cortex (Lange et al. 2004), suggesting the participation of heterotopic cortex to integrated functional networks (Guerrini et al. 2004).

FDG-PET may show hypermetabolism or glucose uptake similar to the normal cortex (Barkovich 2007).

PVNH can be differentiated from subependymal hamartomas occurring in tuberous sclerosis, which are irregular in shape with the long axis perpendicular to the ventricular walls, are iso-hypointense on MRI sequences to white matter and enhance after intravenous infusion of contrast agents.

FSH must be differentiated from tumors, which enlarge the affected hemisphere, and are associated with normal overlying cortex and surrounding edema (Barkovich and Raybaud 2012).

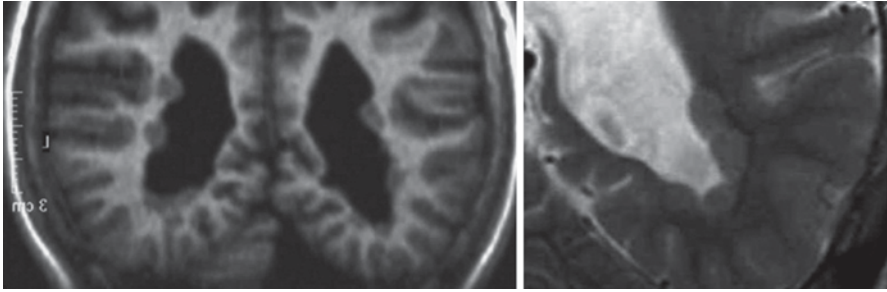


**Fig. 13** T1 3D and enlarged T2 images show heterotopic gray matter nodules of subependymal heterotopia (PVNH)

### Lissencephalies

The term lissencephaly means “smooth brain” and refers to the paucity of gyral and sulcal development on the surface of the brain. In lissencephaly, the cerebral cortex is abnormally thick, usually measuring 10–15 mm (Francis et al. 2006).

Lissencephalies include:

1. classical lissencephaly (type I lissencephaly);
2. subcortical band heterotopia (SBH).

They are part of a malformative complex, the agyria-pachygyria-band spectrum.

Classic lissencephaly may be complete or incomplete with absent (agyria) or decreased (pachygyria) surface convolutions, respectively (Sicca et al. 2003).

CT scan rarely shows small midline septal calcifications (Barkovich 2007).

MRI findings include (Sicca et al. 2003; Barkovich 2007):

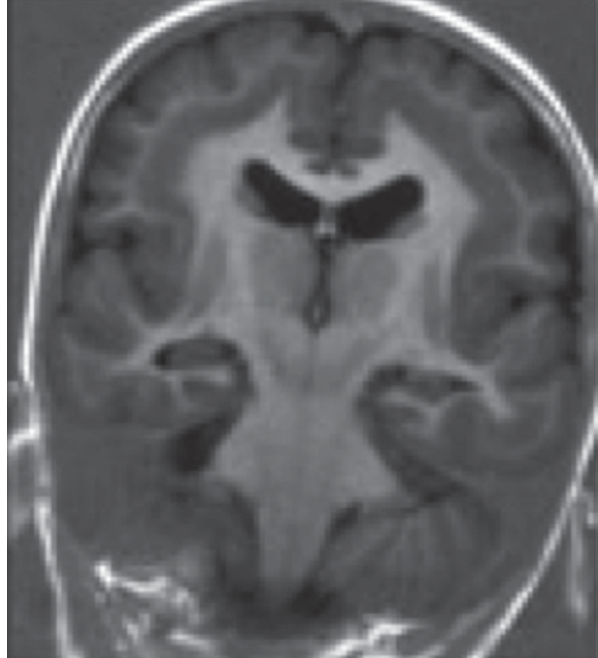
1. smooth brain surface;
2. diminished white matter;
3. shallow and vertically oriented Sylvian fissure, configuring a figure-of-eight appearance of the cerebrum on axial images;
4. the cell-sparse zone, which is a zone of white matter separating a thin outer cortical layer from a thick deeper cortical layer.

Additional abnormalities include: hypoplasia of the corticospinal tracts, heterotopia of the inferior olives, and mild dysplasia of the cerebellar cortex.

On T1w and T2w sequences it is possible to distinguish gray and white matter layers and to identify the cell-sparse zone as areas appearing hypointense in T1w hyperintense in T2w (Barkovich 2007).

SBH is the mildest form of classic lissencephaly. In SBH, the cerebral convolutions appear either normal or mildly broad, but just beneath the cortical ribbon a thin band of white matter separates the cortex from the bands of gray matter (Fig. 14). Band heterotopia may be complete or partial. In T2w sequences, it is sometimes possible to identify foci of hyperintensity in white matter, associated with a poor motor outcome (Gleeson et al. 2000; Mai et al. 2003).

**Fig. 14** Coronal T1 weighted shows subcortical band heterotopia.



MRS may identify decreased levels of NAA in the affected cortex (Barkovich 2007). FDG-PET may show glucose uptake similar to or greater than normal cortex (De Volder et al. 1994).

Differential diagnosis include lissencephaly variants (without cell-sparse zone) and bilateral and diffuse subependymal heterotopia.

### **Tuberous Sclerosis**

Tuberous sclerosis, or tuberous sclerosis complex (TSC), belongs to the group of the phakomatoses and involves primarily the central nervous system, the skin and the kidney (Luat et al. 2007).

The characteristic brain lesions are (Jahodova et al. 2014):

1. cortical tubers;
2. subependymal nodules (SEN);
3. subependymal giant cell astrocytomas (SEGAs);
4. white matter abnormalities.

Cortical tubers are the most characteristic lesions of tuberous sclerosis and they are most commonly supratentorial, appearing as pyramidal-shaped gyral expansions.

On CT scans, cortical tubers in neonates and infants appear hyperdense, while in children and adults they may be difficult to identify if they are not calcified (Kalantari and Salamon 2008).

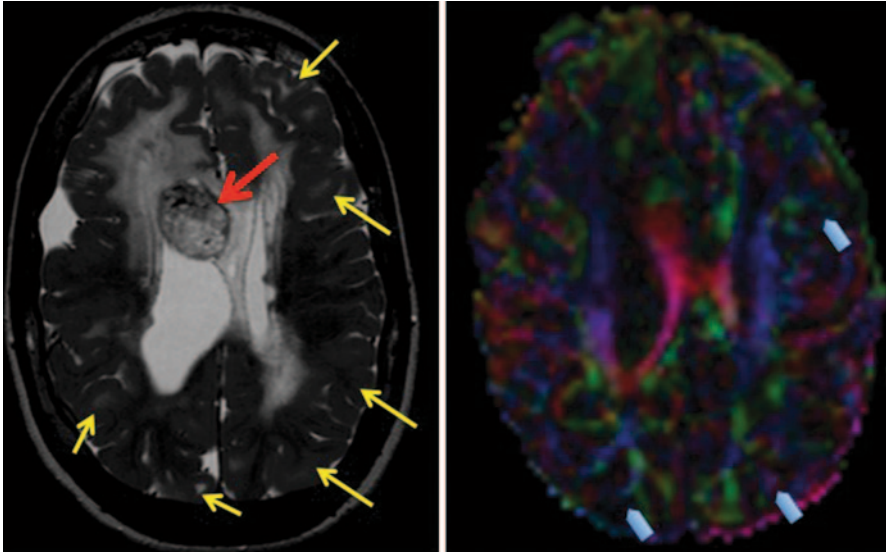


**Fig. 15** Axial T2 weighted and DTI FA color map show subependymal giant cell astrocytoma (SEGA) in the right foramen of Monro (*red arrow*) surrounded by oedema, and multiple cortical tubers (*yellow arrows*). In the DTI FA color map, decreased anisotropy of the tubers (*arrowheads*), compared with normal white matter, can be appreciated

The MRI appearance also changes with ages, as white matter myelinates, and cortical tubers may have different imaging patterns called “gyral core” and “sulcal island”. In neonates they are hyperintense in T1w and hypointense in T2w sequences compared to unmyelinated white matter. In older infants and children, they become hypointense in T1w and hyperintense in T2w and FLAIR sequences, the latter being the most sensitive sequence for the detection of tubers in children and in adults (Kalantari and Salamon 2008).

When cortical tubers calcify, they may appear hyperintense on T1w images. Generally, they do not enhance after administration of contrast medium (Jahodova et al. 2014; Kalantari and Salamon 2008).

On DWI and DTI, they have increased diffusivity and decreased anisotropy compared to normal white matter (Peters et al. 2013 Fig. 15).

MRS has been proposed as a reliable tool for the differential diagnosis of cortical tubers versus neoplasms, especially when cortical tubers are solitary. In cortical tubers, MRS shows normal to slightly elevated levels of choline and slightly diminished levels of NAA, while neoplasms have marked elevation of choline and marked diminution of NAA, with an increased peak of myo-inositol (Kalantari and Salamon 2008; Jahodova et al. 2014). However, low-grade tumors may have MRS findings similar to tubers. In these cases, PWI may be helpful: most cortical tubers are generally hypoperfused compared to gray matter (Jahodova et al. 2014).

SEN are the most common brain hamartomas in tuberous sclerosis. They are more frequently located along the ventricular surface of the caudate nucleus.

On CT scans they may be difficult to identify in infants, but become more easily and progressively detected as they calcify (Barkovich 2007).

On MRI, their appearance changes as the surrounding white matter myelinates. In neonates they are hyperintense on T1w and hypointense on T2w sequences, while they become more isointense to gray matter with age and are better identified on T1w images. If they calcify, they may appear hypointense on T2\*w GE or susceptibility-weighted images. After intravenous administration of contrast material, SEN show variable enhancement; they also have increased diffusivity and reduced fractional anisotropy compared to surrounding white matter (Luat et al. 2007).

SEGA is an enlarged subependymal nodule, usually located near the foramen of Monro. Their incidence in TSC is 5–10% and they may result in a clinical presentation of hydrocephalus, as they tend to enlarge (Barkovich 2007).

On imaging studies, SEGAs are identified by the demonstration of tumor growth on serial studies or by the development of hydrocephalus associated with tumor near the foramen of Monro. They tend to grow into the ventricle and rarely infiltrate the adjacent nervous tissue: in this case, they frequently have degenerated into high-grade neoplasms (Barkovich 2007).

The major differential diagnosis of TSC include subependymal heterotopia, TORCH and Taylor type cortical dysplasia.

## Sturge-Weber Syndrome

Sturge-Weber Syndrome (SWS) is a sporadic phakomatosis characterized by angiomas involving the face (port-wine stain), the choroid of the eye and the leptomeninges. Venous occlusion and ischemia lead to angiomas with cortical calcium deposition and atrophy (Barkovich 2007).

CT findings include gyral and subcortical calcifications, occurring exclusively in brain areas near the angioma (Barkovich 2007).

MRI in patients with Sturge-Weber can show (Juhász et al. 2007b):

1. atrophy;
2. high signal on T2WI due to gliosis;
3. low signal in areas with calcifications;
4. leptomeningeal enhancement (Fig. 16).

On MRI, in neonatal cases, the white matter appears hypointense on T2w images in the affected hemisphere because of “accelerated” myelin maturation. The affected hemisphere becomes progressively atrophic with hyperpneumatization of the paranasal sinuses, thick diploe, and enlarged ipsilateral choroid plexus (Juhász et al. 2007b).

Calcifications may be identified on SWI or T2\*w GE images as a thin ribbon of low signal intensity adjacent to the cerebral cortex in the affected areas. SWI sequences appears superior also in assessing the enlarged transmedullary veins, the pathological periventricular veins and the cortical gyriform abnormalities (Wu et al. 2011).

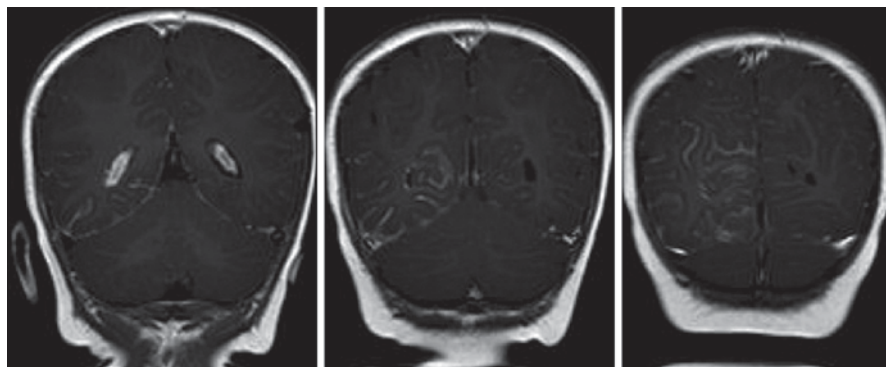


**Fig. 16** Coronal contrast-enhanced T1 of leptomeningeal angiomas involving the right occipital lobe, a feature consistent with Sturge-Weber Syndrome

After gadolinium administration, subcortical, leptomeningeal, and choroidal serpentine T1 hyperintensity is the rule, due to the enhancement of the pial angiomatous malformation mainly localized in the occipital lobes (Barkovich 2007; Juhász et al. 2007a).

PWI may be useful in detecting cerebral hypoperfusion of the brain underlying the enhancing pial angioma, due to impaired venous drainage (Miao et al. 2011).

MRS of the affected brain regions reveals reduced NAA, elevated choline and lactate (Batista et al. 2008).

FDG-PET shows hypermetabolism in the affected area in the early stages with subsequent hypometabolism, and it may be useful in surgical planning of cortical resection for intractable seizures (Juhász et al. 2007a).

For the differential diagnosis, it is important to consider leptomeningeal enhancement and other neurocutaneous syndromes.

### Hemimegalencephaly

Hemimegalencephaly is a rare disease characterized by hamartomatous growth of one cerebral hemisphere or part of it.

Associated findings include macrocephaly and somatic hemihypertrophy of the body.

On CT and MRI, part or all of a hemisphere may be affected (Flores-Sarnat 2002).

The most typical findings are (Kamiya et al. 2013):

1. enlarged hemisphere with ipsilateral ventriculomegaly (Fig. 17);
2. abnormal gyral pattern with broad gyri, shallow sulci, blurring of the cortical-white matter junction and cortical thickening;
3. thickened cortex with a wide spectrum of abnormalities, such as lissencephaly, pachygyria or polymicrogyria;

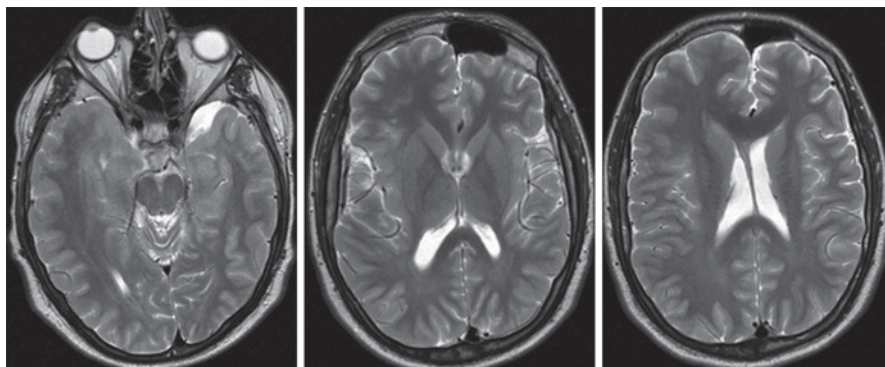


**Fig. 17** Axial T2 weighted images showing right hemimegalencephaly

4. abnormal white matter, frequently hypodense on CT scans and heterogeneous on T2w MRI images, due to heterotopia and dysplastic neurons;
5. resultant midline shift.

In the late stage, the involved hemisphere may be atrophic due to constant seizure activity.

MRS shows reduction of NAA and glutamate peaks in the affected white matter, correlated to a diminished metabolic activity on FDG-PET (Flores-Sarnat 2002).

### **Ganglioglioma**

Gangliogliomas are rare tumors, accounting for 3% of all pediatric brain neoplasms, and 6–7% of supratentorial tumors in children. Affected patients usually present in their second decade of life (Barkovich and Raybaud 2012).

Ganglioglioma typically involves the cortex of the cerebral lobes, especially the temporal lobe (85% of cases), and is the most common tumor associated with temporal lobe epilepsy (Barkovich and Raybaud 2012).

The most typical imaging findings are (Barkovich and Raybaud 2012):

1. presentation as a cyst with enhancing mural nodule (although it may be entirely solid);
2. calcifications in up to 50%.

On CT scan, gangliogliomas appear as hypodense, well circumscribed lesions with calcifications and little edema, typically located within the cerebral cortex. Solid portions of the tumor may appear isodense, hypodense or mixed, with variable contrast enhancement. Erosion of the adjacent inner table of the calvarium may occur when the ganglioglioma is located peripherally (Gelabert-González et al. 2011).

On MRI, the ganglioglioma may have sharply or poorly defined margins. It may be solid, cystic, cystic with mural nodule or multi-cystic. It is usually hyperintense on T2w sequences and heterogeneous on T1w. The solid portion of the lesion may enhance (Barkovich 2012).



Differentiation from DNET and pleomorphic xanthoastrocytoma is difficult and calcifications are important distinguishing factors (Raz et al. 2012).

### **Dysembryoplastic Neuroepithelial Tumor (DNETs)**

DNET are benign lesions of the cerebral cortex and are the cause of 20% of the cases of medically refractory epilepsy in children and young adults (Ozlen et al. 2010).

The key findings on imaging are (Barkovich and Raybaud 2012):

1. swollen gyrus;
2. bubbly cystic appearance;
3. wedge-shaped and pointing toward the ventricle;
4. usually no or only little enhancement;
5. association with focal cortical dysplasia.

On CT studies, DNETs are quite well-demarcated, lobulated cortical lesions hypodense to white matter. Calcifications are present in one third of the cases and erosion of the inner table of the calvarium may be observed (Ozlen et al. 2010).

On MRI, DNET in typical cases present as a bubbly mass which expands the affected gyri. The bubbly cystic appearance is seen as small cyst-like intratumoral structures that are very hyperintense on T2w sequences and hypointense on T1w sequences, with a variable signal on FLAIR images (from hypointense to hyperintense). Diffusivity is elevated compared to the normal gray and white matter. Contrast enhancement is seen in 20–40% of the cases and is usually patchy (Barkovich and Raybaud 2012).

MRS shows no significant difference of the metabolite ratios from normal cortex, while PWI reveals lower CBV than normal cortex (Ozlen et al. 2010; Barkovich and Raybaud 2012).

Furthermore, DNETs are metabolically inactive tumors with no significant glucose uptake on FDG-PET (Barkovich and Raybaud 2012).

### **Hypothalamic Hamartoma (HH)**

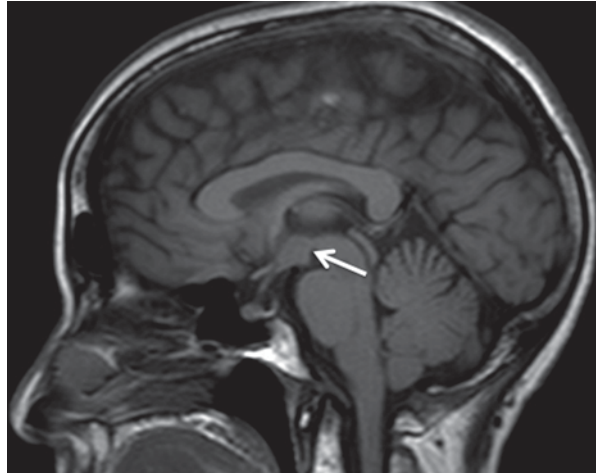
Hypothalamic hamartoma is also known as diencephalic or tuber cinereum hamartoma.

It represents nonneoplastic congenital grey matter heterotopia in the region of tuber cinereum of the hypothalamus. It is seen in infants presenting with epilepsy (gelastic type) and precocious puberty (Mittal et al. 2013; Chung et al. 2012).

A clinical-topographical classification by Valdueza et al. (Valdueza et al. 1994) distinguished 4 types of HH:

1. Ia hamartomas, small lesions with a peduncolated attachment to the tuber cinereum, generally asymptomatic;
2. Ib hamartomas, small peduncolated masses attached to a mammillary body, usually associated to precocious puberty;

**Fig. 18** Sagittal T1 weighted image shows a II A hypothalamic hamartoma (*arrow*)



3. IIa hamartomas, sessile masses (larger than 1.5 cm in diameter) attached to the floor of the third ventricle and mammillary bodies, typically presenting with gelastic seizures;
4. IIb hamartomas, large sessile masses (larger than 1.5 cm in diameter) distorting the walls and the floor of the third ventricle, associated with mental and behavioral disorders in addition to gelastic and mixed epilepsy.

CT studies are sensitive only in detecting large hamartomas, which appear as homogeneous, hypodense rounded masses, without contrast enhancement (Chung et al. 2012).

MRI represents the gold standard imaging modality. The MRI appearance is that of a well defined, round or ovoid mass lying within the hypothalamus (Fig. 18). HH are isointense on T1w sequences compared to gray matter and isointense to slightly hyperintense on T2w images. No enhancement is seen after contrast administration (Amstutz et al. 2006).

Reports in the literature suggest that on MRS the myo-inositol is higher and NAA lower than in the adjacent thalamus, probably due to astrogliosis (Martina et al. 2003).

## References

- Al Sufiani F, Ang LC (2012) Neuropathology of temporal lobe epilepsy. *Epilepsy Res Treat.* vol 2012, Article ID 624519
- Amstutz DR, Coons SW, Kerrigan JF et al (2006) Hypothalamic hamartomas: correlation of MR imaging and spectroscopic findings with tumor glial content. *AJNR Am J Neuroradiol* 27(4):794–798
- Barkovich AJ (2010) Current concepts of polymicrogyria. *Neuroradiology* 52:479–487

- Barkovich AJ, Raybaud C (2012) Pediatric neuroimaging—Fifth edition. Lippincott Williams & Wilkins, Philadelphia
- Barkovich AJ et al (2007) Diagnostic imaging—pediatric neuroradiology. Amrysia
- Batista CE, Chugani HT, Hu J et al (2008) Magnetic resonance spectroscopic imaging detects abnormalities in normal-appearing frontal lobe of patients with Sturge-Weber syndrome. *J Neuroimaging* 18(3):306–313
- Bentivoglio M, Tassi L, Pech E et al (2003) Cortical development and focal cortical dysplasia. *Epileptic Disord* 5(Suppl 2):S27–34
- Berg AT, Testa FM, Levy SR, Shinnar S (2000) Neuroimaging in children with newly diagnosed epilepsy: a community-based study. *Pediatrics* 106:527–532
- Biswal BB (2012) Resting state fMRI: a personal history. *Neuroimage* 62(2):938–944
- Bonilha L, Halford J, Rorden C et al (2007) Microstructural white matter abnormalities in nodular heterotopia with overlying polymicrogyria. *Seizure* 16(1):74–80
- Bronen RA, Fulbright RK, Spencer DD et al (1996) Refractory epilepsy: comparison of MR imaging, CT, and histopathologic findings in 117 patients. *Radiology* 201:97–105
- Caranci F, Bartiromo F, Cirillo L et al (2007) Thalamic changes in mesial temporal sclerosis: a limbic system pathology. *Neuroradiol J* 218–223
- Caruso PA, Johnson J, Thibert R et al (2013) The use of magnetic resonance spectroscopy in the evaluation of epilepsy. *Neuroimag Clin N Am* 23:407–424
- Chugani HT, Shields WD, Shewmon DA et al (1990) Infantile spasms: I. PET identifies focal cortical dysgenesis in cryptogenic cases for surgical treatment. *Ann Neurol* 7(4):406–413
- Chung EM, Biko DM, Schroeder JW et al (2012) From the radiologic pathology archives: precocious puberty: radiologic-pathologic correlation. *Radiographics* 32(7):2071–2099
- Colombo N, Salamon N, Raybaud C et al (2009) Imaging of malformations of cortical development. *Epileptic Disord* 11(3):194–205
- De Cocker L, D’Arco F, Demaerel P, Smithuis R (2012) Role of MRI in epilepsy. *The Radiology Assistant*. [www.radiologyassistant.nl/en](http://www.radiologyassistant.nl/en). Accessed 1 Sept 2012
- De Volder AG, Gadiuseux JF, Michel CJ et al (1994) Brain glucose utilization in band heterotopia: synaptic activity of “double cortex”. *Pediatr Neurol* 11:290–294
- Dumas de la Roque A, Oppenheim C, Chassoux F et al (2005) Diffusion tensor imaging of partial intractable epilepsy. *Eur Radiol* 15:279–285
- Eriksson SH, Rugg-Gunn FJ, Symms MR et al (2001) Diffusion tensor imaging in patients with epilepsy and malformations of cortical development. *Brain* 124:617–626
- Farid N, Girard HM, Kemmotsu N et al (2012) Temporal lobe epilepsy: quantitative MR volumetry in detection of hippocampal atrophy. *Radiology* 26(2):542–550
- Flores-Sarnat L (2002) Hemimegalencephaly: part I. Genetic, clinical, and imaging aspects. *J Child Neurol* 17(5):373–384
- Fonseca Vde C, Yasuda CL, Tedeschi GG et al (2012) White matter abnormalities in patients with focal cortical dysplasia revealed by diffusion tensor imaging analysis in a voxelwise approach. *Front Neurol* 121
- Francis F, Meyer G, Fallet-Bianco C et al (2006) Human disorders of cortical development: from past to present. *Eur J Neurosci* 23:877–893
- Gastaut H, Gastaut JL (1979) Computerized transverse axial tomography in epilepsy. *Epilepsia* 17:325–336
- Gelabert-González M, Amo JM, Arcos Algaba A et al (2011) Intracranial gangliogliomas. A review of a series of 20 patients. *Neurologia* 26(7):405–415
- Gleeson JG, Luo RF, Grant PE et al (2000) Genetic and neuroradiological heterogeneity of double cortex syndrome. *Ann Neurol* 47:265–269
- Guerrini R, Marini C (2006) Genetic malformations of cortical development. *Exp Brain Res* 173(2):322–333
- Guerrini R, Mei D, Sisodiya S et al (2004) Germline and mosaic mutations of FLN1 in men with periventricular heterotopia. *Neurology* 63:51–56

- Guimaraes CA, Bonilha L, Franzon RC et al (2007) Distribution of regional gray matter abnormalities in a pediatric population with temporal lobe epilepsy and correlation with neuropsychological performance. *Epilepsy Behav* 11:558–566
- Hankey G, Davies L, Gubbay SS (1989) Long term survival with early childhood intracerebral tumours. *J Neurol Neurosurg Psychiatry* 52:778–781
- Iaccarino C, Tedeschi E, Rapan  A et al (2009) Is the distance between mammillary bodies predictive of a thickened third ventricle floor? *J Neurosurg* 110(5):852–857
- Jahodova A, Krsek P, Kyncl M et al (2014) Distinctive MRI features of the epileptogenic zone in children with tuberous sclerosis. *Eur J Radiol* 83(4):703–709
- Juh sz C, Batista CE, Chugani DC et al (2007a) Evolution of cortical metabolic abnormalities and their clinical correlates in Sturge-Weber syndrome. *Eur J Paediatr Neurol Sep*; 11(5):277–284
- Juh sz C, Haacke EM, Hu J et al (2007b) Multimodality imaging of cortical and white matter abnormalities in Sturge-Weber syndrome. *AJNR Am J Neuroradiol* 28(5):900–906
- Kalantari BN, Salamon N (2008) Neuroimaging of tuberous sclerosis: spectrum of pathologic findings and frontiers in imaging. *AJR Am J Roentgenol* 190(5):W304–309
- Kamiya K, Sato N, Saito Y et al (2013) Accelerated myelination along fiber tracts in patients with hemimegalencephaly. *J Neuroradiol* 30. pii: S0150-9861(13)00084-9. doi:10.1016/j.neurad.2013.08.005. (Epub ahead of print)
- Keller SS, Roberts N (2007) Voxel-based morphometry of temporal lobe epilepsy: an introduction and review of literature. *Epilepsia* 49(5):741–757
- Lange M, Winner B, Muller JL et al (2004) Functional imaging in periventricular nodule heterotopy caused by a new Filamin A mutation. *Neurology* 62:151–152
- Lee MJ, Kim HD, Lee JS, Kim DS, Lee SK (2013) Usefulness of diffusion tensor tractography in pediatric epilepsy surgery. *Yonsei Med J* 54(1):21–27
- Li LM, Cendes F, Bastos AC et al (1998) Neuronal metabolic dysfunction in patients with cortical developmental malformations. A proton magnetic resonance spectroscopic imaging study. *Neurology* 50:755–759
- Li Y, Du H, Xie B et al (2010) Cerebellum abnormalities in idiopathic generalized epilepsy with generalized tonic-clonic seizures revealed by diffusion tensor imaging. *PLoS One* 5(12):e15219
- Li Q, Zhang Q, Sun H, Zhang Y, Bai R (2011) Double inversion recovery magnetic resonance imaging at 3 T: diagnostic value in hippocampal sclerosis. *J Comput Assist Tomogr* 35(2):290–293
- Lim CC, Yin H, Loh NK, Chua VG et al (2005) Malformations of cortical development: high-resolution MR and diffusion tensor imaging of fiber tracts at 3T. *AJNR Am J Neuroradiol* 26(1):61–64
- Luat AF, Makki M, Chugani HT (2007) Neuroimaging in tuberous sclerosis complex. *Curr Opin Neurol* 20(2):142–150
- Luo C, Li Q, Lai X et al (2011) Altered functional connectivity in default mode network in absence epilepsy: a resting-state fMRI study. *Hum Brain Mapp* 32:438–449
- Mai R, Tassi L, Cossu M et al (2003) A neuropathological, stereo-EEG, and MRI study of subcortical band heterotopia. *Neurology* 60:1834–1838
- Marsh I, Lim Ko, Sullivan EV et al (1996) Proton magnetic resonance spectroscopy of a gray matter heterotopia. *Neurology* 47:1571–1574
- Martina DD, Seeger U, Ranke MB, Grodd W (2003) MR imaging and spectroscopy of a tuber cinereum hamartoma in a patient with growth hormone deficiency and hypogonadotropic hypogonadism. *AJNR Am J Neuroradiol* 24:1177–1180
- Miao Y, Juh sz C, Wu J et al (2011) Clinical correlates of white matter blood flow perfusion changes in Sturge-Weber syndrome: a dynamic MR perfusion-weighted imaging study. *AJNR Am J Neuroradiol* 32(7):1280–1285
- Milligan TA, Zamani A, Bromfield E (2009) Frequency and patterns of MRI abnormalities due to status epilepticus. *Seizure* 18(2):104–108
- Mittal S, Mittal M, Montes JL et al (2013) Hypothalamic hamartomas. Part 1. Clinical, neuroimaging, and neurophysiological characteristics. *Neurosurg Focus* 34(6):E6

- Montenegro MA, Li LM, Guerreiro MM et al (2002) Focal cortical dysplasia: improving diagnosis and localization with magnetic resonance imaging multiplanar and curvilinear reconstruction. *J Neuroimaging* 12:224–230
- Mueller SG, Ebel A, Barakos J et al (2011) Widespread extrahippocampal NAA/(Cr + Cho) abnormalities in TLE with and without mesial temporal sclerosis. *J Neurol* 258(4):603–612
- Opplet A (2006) Imaging systems for medical diagnostics. fundamentals, technical solutions and applications for systems applying ionizing radiation, nuclear magnetic resonance and ultrasound. Siemens, 2006
- Osborn AG (2013). *Osborn's brain: imaging, pathology, and anatomy*. Amysis Salt Lake City, Utah
- Ozlen F, Gunduz A, Asan Z et al (2010) Dysembryoplastic neuroepithelial tumors and gangliogliomas: clinical results of 52 patients. *Acta Neurochir (Wien)* 152(10):1661–1671
- Peters JM, Taquet M, Prohl AK et al (2013) Diffusion tensor imaging and related techniques in tuberous sclerosis complex: review and future directions. *Future Neurol* 8(5):583–597
- Pittau F, Grouiller F, Spinelli L et al (2014) The role of functional Neuroimaging in pre-surgical epilepsy evaluation. *Front Neurol* 5:31
- Raz E, Zagzag D, Saba L et al (2012) Cyst with a mural nodule tumor of the brain. *Cancer Imaging* 12:237–244
- Savic I, Thomas AM, Ke Y et al (2000) In vivo measurements of glutamine + glutamate (Glx) and N-acetyl aspartate (NAA) levels in human partial epilepsy. *Acta Neurol Scand* 102:179–188
- Scott CA, Fish DR, Smith SJ et al (1999) Presurgical evaluation of patients with epilepsy and normal MRI: role of scalp video-EEG telemetry. *J Neurol Neurosurg Psychiatry* 66:69–71
- Sicca F, Kelemen A, Genton P et al (2003) Mosaic mutations of the LIS1 gene cause subcortical band heterotopia. *Neurology* 61:1042–1046
- Striano P, Caranci F, Di Benedetto R et al (2009) <sup>1</sup>H MR spectroscopy indicates prominent cerebellar dysfunction in benign adult familial myoclonic epilepsy. *Epilepsia* 50(6):1491–1497
- Trishit Roy T, Alak Pandit (2011) Neuroimaging in epilepsy. *Ann Indian Acad Neurol* 14(2):78–80
- Valdueva JM, Cristante L, Dammann O et al (1994) Hypothalamic hamartomas: with special reference to gelastic epilepsy and surgery. *Neurosurgery* 34(6):949–958
- Wattjes MP, Lutterbey GG, Gieseke J et al (2007) Double Inversion Recovery brain imaging at 3T: diagnostic value in the detection of multiple sclerosis lesions. *AJNR Am J Neuroradiol* 28:54–59
- Widjaja E, Raybaud C (2008) Advances in neuroimaging in patient with epilepsy. *Neurosurg Focus* 25(3):E3
- Widjaja E, Zarei S, Mahmoodabadi CG et al (2012) Reduced cortical thickness in children with new-onset seizures. *AJNR Am J Neuroradiol* 33:673–677
- Widjaja E, Zamyadi M, Raybaud C et al (2013) Abnormal functional network connectivity among resting-state networks in children with frontal lobe epilepsy. *AJNR Am J Neuroradiol* 4:2386–2392
- Widjaja E, Kis A, Go C et al (2014) Bilateral white matter abnormality in children with frontal lobe epilepsy. *Epilepsy Res* 108(2):289–294
- Wieck G, Leventer RJ, Squier WM et al (2005) Periventricular nodular heterotopia with overlying polymicrogyria. *Brain* 128(Pt 12):2811–2821
- Wintermark P, Lechpammer M, Warfield SK et al (2013) Perfusion imaging of focal cortical dysplasia using Arterial Spin Labeling: correlation with histopathological vascular density. *J Child Neurol* 28(11):1474–1482
- Wolf RL, Alsop DC, Levy-Teis I et al (2001) Detection of mesial temporal lobe hypoperfusion in patients with temporal lobe epilepsy by use of arterial spin labeled perfusion MR imaging. *AJNR Am J Neuroradiol* 22(7):1334–1341
- Wu J, Tarabishy B, Hu J et al (2011) Cortical calcification in Sturge-Weber syndrome on MRI-SWI: relation to brain perfusion status and seizure severity. *J Magn Reson Imaging* 34(4):791–798
- Wyllie E, Rothner AD, Luders H (1989) Partial seizures in children. Clinical features, medical treatment, and surgical considerations. *Pediatr Clin North Am* 36:343–364